SUPPLEMENTARY MATERIAL 1 TO THE WESTERN HUDSON BAY POLAR BEAR AERIAL SURVEY REPORT

Analysis of the 2011 data set using the LANDSAT habitat covariate

Comparison of the distribution of detections from 2011 and 2016 revealed a larger range of detections at further distances in 2016 compared to 2011. One potential reason for this was likely the lower visibility in 2011 as indicated by 68% (n=100 of 147 observations) of observations with a visibility rating of 1 indicating "fair" visibility. In contrast, only 8.4% (15 of 178) observations had a fair visibility rating in 2016 (Figure SM1.1). We right truncated the 2011 distance at 1800 meters as was done in previous analyses (Stapleton et al. 2014).

The distribution of *RSveg* remote sensing habitat classes was well distributed for all 5 habitat classes with more observations closer to the transect line for all categories. For this reason the full *RSveg* habitat class was considered in addition to the *RSveg2* class (which pooled shrub and low vegetation), used in the 2016 analysis, which pooled the shrub and low vegetation class (Figure SM1.2). The 2011 survey used a "structure" covariate to describe sightability rather than habitat classes with 0 indicating no obstruction and 1 indicating obstruction by vegetation. There was a slight pattern where most of the obstructed observations occurred in the low vegetation and shrub category. There were less observations for the tree category which may have been due to reduced visibility in these areas. The gravel category had few observations with obstruction. Models were considered which had both the *RSveg* and *structure* covariates under the assumption that each covariate was describing different factors influencing sightability. For example, it is possible that the structure covariate was describing small-scale factors influencing sightability whereas the *RSveg* class was describing large scale factors.

Model selection results suggested support for a model with *RSveg2* habitat covariate, visibility, and the structure covariate with a hazard rate detection function (Table SM1.1, model 1). Also supported was a model with the full *RSveg* categories (shrub and low vegetation not pooled) with structure and visibility. This model was more supported than a half normal model with structure and visibility which was supported in the previous analysis (Stapleton et al. 2014). The estimate of abundance from model 1 (955) was higher than the half-normal structure/visibility model (model 5; 912).

Goodness of fit tests for the most supported model (model 1, Table SM1.1) suggested adequate fit (χ^2=6.15, df=4,p=0.18). Kolmogorov-Smirnov tests (0.034, p=0.99) and Cramer-Von-Mises tests (0.02, p=0.99) also suggested fit was adequate. The model averaged estimate of abundance from all model in Table SM1 was 949 bears (SE=168.9, CI=618-1280, CV=17.7%), If the *RSveg* models were removed from the analysis then the estimate was 914 (SE=162.6, CI=596-1232 ,CV=17.7%) which was close to the model averaged estimate from the previous analysis (Stapleton et al. 2014) of the coastal and inland zones (929, SE=186).

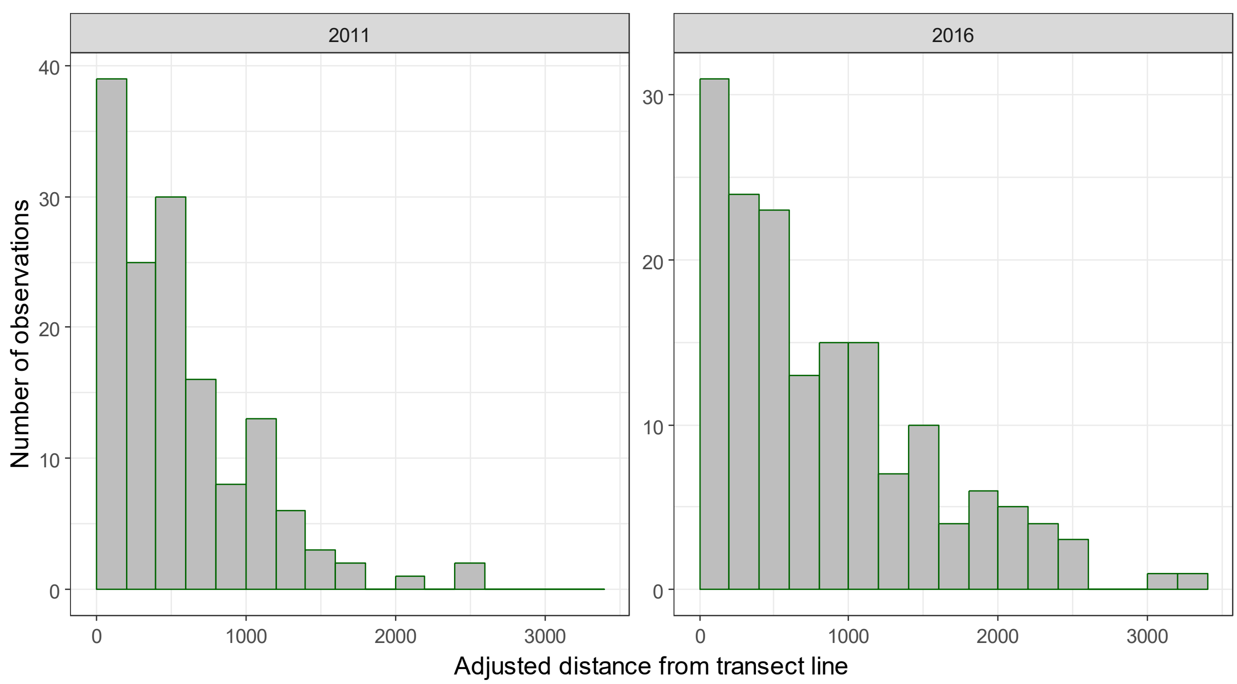

Figure SM1.1: A comparison of the distribution of detections for 2011 and 2016 surveys.

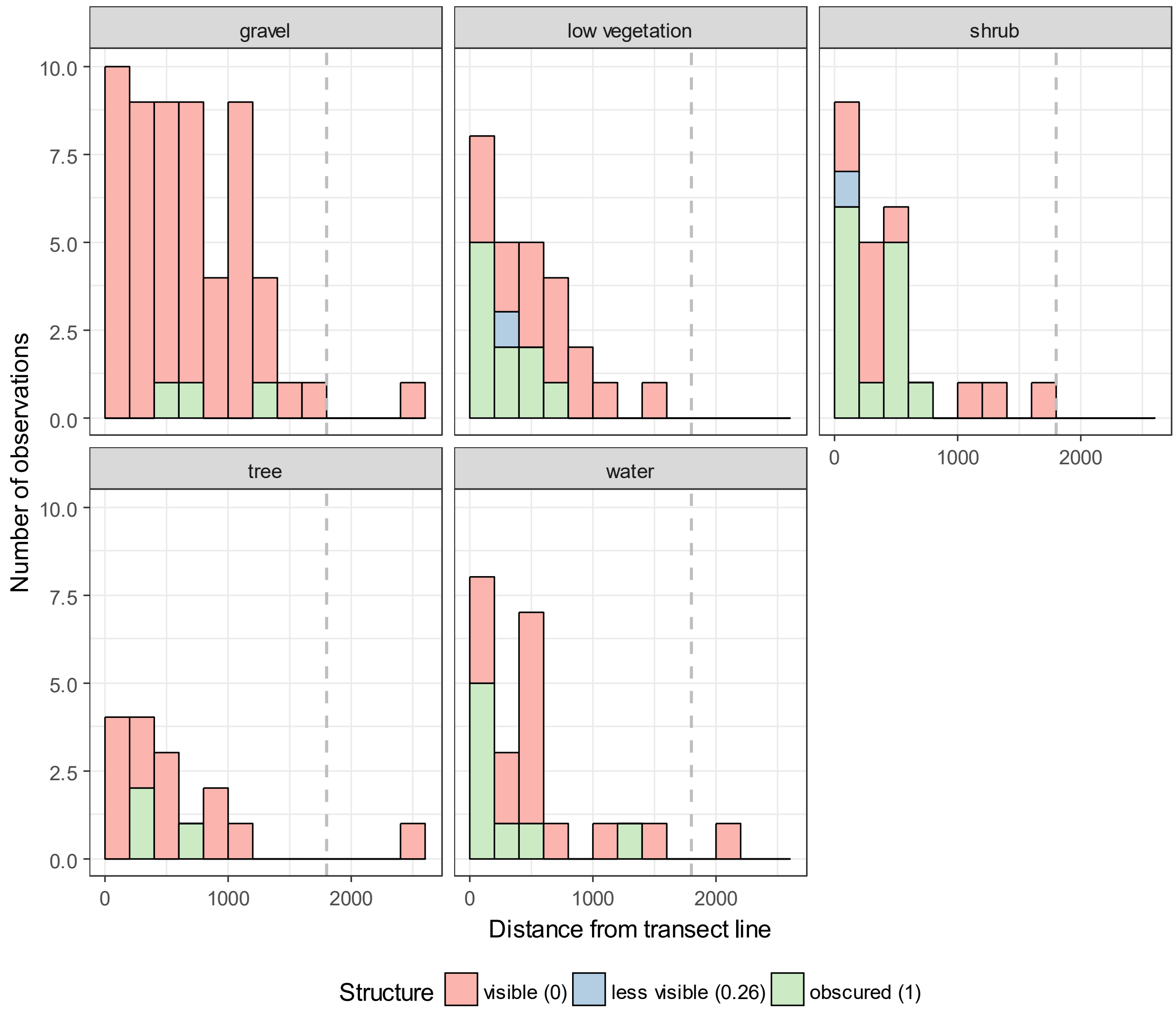

Figure SM1.2: The distribution of the remote sensing based habitat classes (*RSveg*) for the 2011 survey. The structure covariate used to describe whether observations were obscured is shown as sub bars for comparison purposes. The left truncation distance of 1800 used in the 2011 survey is shown as a vertical line.

Table SM1.1: Model selection results for 2011 Hudson Bay distance sampling analysis. Akaike information criterion (AIC), the differences between AIC of the given model and most supported model ΔAIC, Akaike weight (w_i), and Log-likelihood of each model is also shown.

No	DF	Covariates	AIC	ΔAIC	w_i	K	LogL	N	Conf. Limit		CV
1	HR	RSveg2+vis+structure	2060.49	0.00	0.47	7	-1023.2	955	675	1350	17.7%
2	HR	RSveg+vis+structure	2062.40	1.91	0.18	8	-1023.2	948	671	1338	17.6%
3	HR	RSveg2+vis	2062.59	2.10	0.16	6	-1025.3	953	670	1355	18.0%
4	HR	RSveg+vis	2064.59	4.10	0.06	7	-1025.3	953	670	1354	18.0%
5	HN	structure+vis	2064.91	4.41	0.05	3	-1029.5	912	655	1270	16.9%
6	HN	RSveg+vis	2066.10	5.61	0.03	6	-1027.0	951	680	1330	17.1%
7	HN	structure+vis+size	2066.79	6.30	0.02	4	-1029.4	894	643	1244	16.8%
8	HR	structure+vis	2067.85	7.36	0.01	4	-1029.9	932	650	1338	18.5%
9	HR	structure+vis+size	2068.99	8.50	0.01	5	-1029.5	990	645	1520	22.0%
10	HN	structure	2069.73	9.24	0.00	2	-1032.9	875	635	1206	16.4%
11	HR	RSveg nowater+vis	2070.28	9.79	0.00	6	-1029.1	936	648	1353	18.8%
12	HN	structure+size	2071.48	10.99	0.00	3	-1032.7	903	636	1281	17.9%
13	HR	structure+size	2074.20	13.71	0.00	4	-1033.1	949	636	1416	20.5%
14	HR	Rsveg-hab	2075.31	14.82	0.00	5	-1032.7	915	641	1308	18.3%
15	HR	RSveg2	2075.55	15.06	0.00	5	-1032.8	864	614	1216	17.5%
16	HR	RSveg	2076.74	16.25	0.00	6	-1032.4	883	624	1249	17.7%
17	HN	constant	2077.36	16.87	0.00	1	-1037.7	852	608	1195	17.2%
18	HN	RSveg	2078.07	17.58	0.00	5	-1034.0	869	628	1203	16.6%
19	HN	size	2079.35	18.86	0.00	2	-1037.7	856	601	1221	18.1%
20	HR	constant	2079.75	19.26	0.00	2	-1037.9	869	602	1255	18.8%
21	HR	size	2081.71	21.22	0.00	3	-1037.9	905	604	1356	20.7%